University of Baghdad
College of Engineering
JE
JOURNAL OF ENGINEERING

Journal of Engineering

journal homepage: www.joe.uobaghdad.edu.iq

Volume 30 Number 2 February 2024

Performance Evaluation of Two Stages Parallel Flow Indirect Evaporative Cooling with Aspen Pads in Baghdad Climate Conditions

Hassan Farid Garbi[1,*], Najim A. Jassim[2]

Department of Mechanical Engineering, College of Engineering, University of Baghdad, Baghdad, Iraq
hassan.nasser2003m@coeng.uobaghdad.edu.iq[1], Najmosawe@yahoo.com[2]

ABSTRACT

This study delves into the realm of advanced cooling techniques by examining the performance of a two-stage parallel flow indirect evaporative cooling system enhanced with aspen pads in the challenging climate of Baghdad. The objective was to achieve average air dry bulb temperatures (43 °C) below the ambient wet bulb temperatures (24.95 °C) with an average relative humidity of 23%, aiming for unparalleled cooling efficiency. The research experiment was carried out in the urban environment of Baghdad, characterized by high temperature conditions. The investigation focused on the potential of the two-stage parallel flow setup, combined with the cooling capability of aspen pads, to surpass the limitations imposed by conventional cooling methods. The empirical findings underscored the capacity of the two-stage parallel flow configuration to achieve air-dry bulb temperatures surpassing the ambient wet bulb temperature.

Nonetheless, it was evident that an excessive application of water (exceeding 9 lpm) onto the aspen pads within the wet channels yielded adverse repercussions on the cooler's performance metrics, specifically in terms of wet bulb effectiveness and coefficient of performance. A range of air flows spanning from 150 CMH to 350 CMH was analyzed, revealing the influence of heightened air flow rates on the resultant dry bulb temperatures delivered by the cooling system. Notably, the peak wet-bulb effectiveness registered at 1.08, concurrently yielding a coefficient of performance measuring 7.8.

Keywords: Indirect evaporative cooling, Parallel flow, Sub-wet bulb temperature.

*Corresponding author
Peer review under the responsibility of University of Baghdad.
https://doi.org/10.31026/j.eng.2024.02.05

Article received: 29/06/2023
Article accepted: 19/11/2023
Article published: 01/02/2024

تقييم أداء التبريد التبخيري غير المباشر بالتدفق المتوازي على مرحلتين باستخدام منصات الحور الرجراج في مناخ بغداد

حسن فريد غربي ناصر*, نجم عبد جاسم

قسم الهندسة الميكانيكية، كلية الهندسة، جامعة بغداد، بغداد، العراق

الخلاصة

تتعمق هذه الدراسة في مجال تقنيات التبريد المتقدمة من خلال فحص أداء نظام التبريد التبخيري غير المباشر ذو التدفق المتوازي ذو المرحلتين والمعزز بمنصات الحور الرجراج في مناخ بغداد الصعب. وكان الهدف هو تحقيق درجات حرارة الهواء الجاف (43 درجة مئوية) أقل من درجات حرارة اللمبة الرطبة المحيطة (24.95 درجة مئوية)، بهدف تحقيق كفاءة تبريد عالية. أجريت التجربة البحثية في البيئة الحضرية لمدينة بغداد والتي تتميز بظروف درجات الحرارة المرتفعة. ركز البحث على إمكانية إعداد التدفق المتوازي على مرحلتين، جنبًا إلى جنب مع قدرة التبريد لمنصات الحور الرجراج ، لتجاوز القيود التي تفرضها طرق التبريد التقليدية. أكدت النتائج التجريبية قدرة التدفق المتوازي ذو المرحلتين على تحقيق درجات حرارة الهواء الجاف دون درجة حرارة المصباح الرطب المحيط. ومع ذلك، كان من الواضح أن الاستخدام المفرط للمياه (يتجاوز 9 لتر في الدقيقة) على منصات الحور الرجراج داخل القنوات الرطبة أدى إلى تداعيات سلبية على مقاييس أداء المبرد، وتحديدًا من حيث فعالية اللمبة الرطبة ومعامل الأداء. تم إخضاع مجموعة من تدفقات الهواء من 150 سم مكعب في الساعة إلى 350 سم مكعب في الساعة للتحليل، مما يكشف عن تأثير معدلات تدفق الهواء المرتفعة على درجات حرارة اللمبة الجافة الناتجة التي يوفرها نظام التبريد. ومن الجدير بالذكر أن ذروة فعالية اللمبة الرطبة سجلت 1.08، مما أدى في الوقت نفسه إلى تحقيق معامل أداء يبلغ 7.8.

الكلمات المفتاحية: التبريد التبخيري غير المباشر ، التدفق المتوازي ، دون درجة حرارة البصيلة الرطبة.

1. INTRODUCTION

Indirect evaporative cooling (IEC) is the optimal approach to achieve lowered dry bulb temperatures in supplied air without concurrent moisture content elevation **(Duan et al., 2012; Bogdan et al., 2015)**. This method enables the attainment of dry bulb temperatures beneath both the wet bulb temperature and dew point, positioning it as a formidable contender for efficient cooling. Comprising dual dry and wet channels demarcated by a thin, high-conductivity material, typically aluminum. The cooling process is executed through water dispersion within the wet channel via nozzles. This operation facilitates air cooling while engendering a heat exchange between the dry and wet channels while preserving the moisture content of the air within the dry channel **(Boukhanouf et al., 2013)**. Characterized by its efficiency and cooling prowess, sub-wet bulb temperature IEC emerges as an exemplary solution, potentially lowering the dry bulb temperature of supplied air below the ambient wet bulb temperature **(Bai et al., 2020; Hashim et al., 2022)**. Typically implemented across two stages, this method mandates a sizable cooler configuration.

(Kheirabadi, 2000; Hajidavalloo, 2007) found that evaporative cooling is appropriate for hot areas with little humidity. In dry climates, the cost and operation of evaporative cooling systems are much less than that of traditional cooling systems (Ac), equal to 80%. Using the method of evaporating water droplets for the purpose of carrying out the cooling process is often less energy consuming than traditional air conditioning systems **(Najam and Firas, 2014)**. Still, the problem of increasing the moisture content of supplied air remains the first obstacle when thinking about using direct evaporative cooling. Therefore, it was directed to indirect evaporative cooling, which works by an exact mechanism.

Recently, there have been requests for research and studies on non-simple two-stage evaporative cooling systems using air flow methods (**Shubha et al., 2021**). **(El-Dessouky et al., 2004)** conducted a laboratory test investigation of an indirect/direct evaporative cooling system. The water is sprayed through nozzles on a cooling medium, has thicknesses of 0.1 m, 0.2 m, and 0.4 m, and is made of polyethylene. The water is pumped from the direct evaporative cooling basin into two heat exchanger tubes before the cooling medium to indirectly increase air exposure to cold spaces without increasing humidity. The results show that the system efficiency was 90-120%, the provided air-dry bulb temperature is less than the wet bulb temperature of surrounding air, and the greater the thickness of the cooling medium, the higher the efficiency of the direct part of evaporative cooling. **(Zhao et al., 2008)** conducted a complete numerical investigation of a sub-wet bulb temperature evaporative cooler, and the investigators offered a variety of design settings to enhance performance, including air velocity range, air passage height, air passage length to height ratio, and flow rates. The thermal performance of the entire system was assessed by calculating wet bulb efficiency, which was determined to be as high as 1.3.

(Heidarinejad et al., 2009) experimentally determined basic operating parameters of an evaporative cooling two-stage system. The system was tested in different ambient air temperatures and at other times of the day up to above 40 ^{o}C and with variable relative humidity. The results showed that the wet bulb effectiveness of indirect evaporative cooling of one stage is between 55-61% and wet bulb effectiveness of the two-stage together (indirect /direct) is between 108-111%, the maximum COP is 9.06, and water consumption in the first stage is less than two-stage together (indirect/direct) by 55%. An experimental study of the Indirect Evaporative Cooling (IEC) system cooler was carried out by **(Lee and Lee, 2013)**. The cooler, 550 cm in length, 690 cm in width, and 350 cm in height, contains channels for dry and wet air, and both channels include fins to increase the surface area for heat transfer, as these fins are made of aluminum and brass. The dry bulb temperature of the air supply was obtained within 22 ^{o}C, which is lower than the ambient air wet bulb temperature, and the wet bulb effectiveness was between 0.72 and 0.92.

(Xu et al., 2016) has experimentally studied the performance of indirect evaporative cooling coolers using seven types of cooling medium, including one pad of traditional kraft paper and six pads of fabric. **(Alklaibi, 2015)** investigated the performance of an internal two-stage evaporative cooler compared to a direct evaporative cooler. Furthermore, he theoretically studied the performance of an interior two-stage evaporative cooler compared to direct evaporative coolers and exterior two-stage evaporative coolers. He established that the efficiency of the internal evaporative cooler was less susceptible to air speed than the efficiency of the direct evaporative cooler. His findings also revealed that the air mass flow rate of the internal evaporative cooler had a higher humidity content than the direct evaporative cooler. **(Kashyap et al., 2020)** experimentally tested the IEC system of counterflow regenerative cooler and compared it with traditional direct evaporative cooling. The experiment was conducted at 45 ^{o}C temperature and 17% relative humidity. The results

concluded that the dry-bulb temperature of air provided by counter flow regenerative cooling was 24.5 °C. In the case of direct evaporative cooling, it was 26 °C. However, decreasing cooling capacity and increasing air velocity in the dry channel leads to a decrease in efficiency and an increase in cooling capacity, and the temperature of supplied water plays a significant role in the case of indirect evaporative cooling of the counterflow regenerative type. **(Riangvilaikul and Kumar, 2010)** gave the experimental findings for a sensible evaporative cooling system for diverse input air conditions (temperature, humidity, and velocity) spanning dry, temperate, and humid regions. The data demonstrate that wet bulb efficiency was high, ranging from 92% to 114%.

(Hasan, 2010) studied a mathematical model to test the IEC system's performance of four flow conditions. The IEC system consists of two stages with three types of flow (parallel flow, counter flow, and combined parallel-regenerative flow). The fourth type consists of a single-stage counterflow regenerative IEC. The results showed a noticeable difference in wet bulb effectiveness and supply air temperature when the inlet was 30 °C ambient temperature and 34% relative humidity. The three cases with two stages (parallel flow, counter flow, and combined parallel-regenerative flow) have wet bulb effectiveness of 109%, 126%, and 131%, respectively. The supplied air temperature was 17.8 °C, 15.9 °C, and 15.3 °C, respectively. As for the fourth type, with a single-stage counterflow regenerative, the wet bulb effectiveness was 116%, and the supplied air temperature was 17 °C. Also, analysis of single-stage counterflow regenerative IEC using a modified ϵ-NTU method **(Hasan, 2012)**.

(Kanzari et al., 2013) studied a mathematical IEC system model that supplies air at a sub-wet bulb temperature using a porous ceramic cooling medium. This material is characterized by its availability in different sizes and types and its structural stability. A one-dimension model was used to numerically determine the complete distribution of temperature, enthalpy, and relative humidity using MATLAB program with finite difference method. According to the result, wet bulb effectiveness for supplied air is 1.23 at 45 °C ambient temperature and 30% relative humidity, with a maximum cooling capacity of 120 W/m^2.

A two-stage evaporative cooling system was experimentally studied for a residential building **(Ali and Issam, 2019)**. The indirect part consists of two heat exchangers consisting of a cooling coil, where water flows through them, which is pumped from the ground (using geothermal water) by a water pump. The direct stage consists of three pads (each pad thickness) of 3 cm. Two pads and one pad are used according to the case studied, and these pads are made of cellulose that is widely available commercially. The results showed that increasing the number of cooling pads leads to an increase in the total efficiency of the cooler by 29.34% and that the total efficiency of the cooler is 167%, where the maximum difference in temperature is 26.2 °C between ambient air and supplied air when using three pads. Still, when using one pad, the difference was about 14.9 °C.

(Taleb and Nima, 2021) studied numerically and experimentally tested the performance of a direct evaporative cooling system using an aluminum foil with a thickness of 0.1 mm as a cooling medium. Several air flow levels between 300-600 CFM and several types of water flows (1.75, 2.5, and 4.5 lpm) were used at an ambient temperature of 45 °C and 23% relative humidity. Good practical results were compared with the numerical results obtained using the ANSYS Fluent program with a small error rate. From experimental results, the relative humidity of air supplied was lower by 57% compared to the commercial cooling pads, with the dry-bulb temperature reaching around 27 °C at a water flow rate of 1.75 lpm. **(Zhou et al., 2021)** studied a novel system called the Thermoelectric-Indirect Evaporative Cooling (TIEC) system is proposed. It combines indirect evaporative cooling with thermoelectric

cooling technology. The TIEC system addresses this by using thermoelectric modules to lower the dry channel surface temperature, reducing the likelihood of condensation. A numerical model is developed to analyze this system, considering condensation from the primary air. Results show that while condensation decreases dew point effectiveness by up to 45.0% due to weakened sensible heat transfer, it increases the coefficient of performance by up to 62.2% by enhancing latent heat transfer.

(Boukhanouf et al., 2017) studied numerically and experimentally the wet bulb effectiveness of an indirect evaporative cooling cooler. The cooler consists of a single stage and is based on porous ceramic material as a cooling medium for water evaporation. The system proved its wet bulb effectiveness in cooling was 1.02, and the cooling capacity was 225 W/m^2 when primary air in the dry channel reached a dry bulb temperature lower than ambient air wet bulb temperature. **(Ali and Issam, 2021)** studied an innovative indirect/direct evaporative cooling system (IDEC) powered by photovoltaic (PV) panels and utilized underground water to assess the IDEC system's performance. The IDEC configuration comprises two cooling coils for indirect evaporative cooling (IEC), succeeded by three cellulose pads for direct evaporative cooling (DEC). Findings reveal that an IDEC system featuring 2 cooling coils and 3 cellulose pads (3 mm thick with a well water flow rate of 5 L/min) exhibits significant temperature differences (14.9 °C, 18.5 °C, 26.2 °C) and enhances IEC efficiency by 81.88%, 82.73%, and 86.57%, respectively. This leads to an overall IDEC system efficiency enhancement of 118%, 125%, and 167%, correspondingly. Underground water decreases PV panel temperatures by approximately 20 °C, resulting in a 24% boost in power production. This innovative IDEC system offers a solution for thermal comfort in hot, dry regions while ensuring energy savings.

The primary objective of the current experimental investigation is to facilitate the reduction of ambient air temperatures during the summer season to levels that fall below the wet bulb temperature of the encompassing atmosphere. This endeavour is achieved by utilizing aspen cooling pads within an indirect evaporative cooling system comprising two stages operating in a parallel flow configuration. The study is specifically geared towards a comprehensive analysis of the thermal efficiency of this cooling apparatus. This analysis encompasses key performance metrics, including cooling capacity, coefficient of performance, wet bulb effectiveness, and water consumption. Through a systematic examination of these parameters, the research endeavours to provide valuable insights into the operational capabilities and efficiency of the cooling system, thereby contributing to the advancement of cooling technologies and sustainable thermal management practices.

2. MATERIALS AND METHOD

2.1 System Description

The air wind tunnel was designed and manufactured to conduct the practical part of this study, and the wind tunnel is entirely made of transparent acrylic with a thickness of 8 mm. The system consists of a centrifugal backward curved direct drive fan with static pressure 570 Pa and rotational speed 2600 rpm **(Nanyoo, 1987)**, where the air is pushed through a duct with a cross-sectional area of (22x22) cm with an airflow rate reaching 350 CMH. The air wind tunnel consists of two main stages to conduct the indirect evaporative cooling process for a two-stage parallel flow **Fig. 5**, through ten dry and ten wet channels, where water pumps spray water with different flows on the aspen pad. The cold air is collected

from the dry channels and redirected to the second stage for additional cooling of this air without increasing the moisture content of the final air supplied.

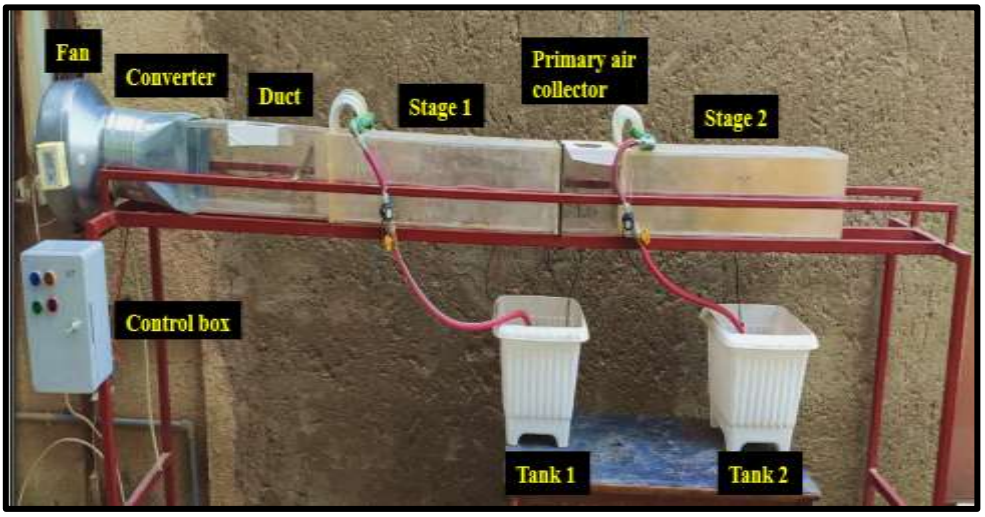

Figure 1. The experimental rig.

2.2 Aluminum Sheets Fabrication Process

One thousand fifty aluminum sheets were used to separate the dry and wet channels **Fig. 2**. This type of aluminum is characterized by high thermal conductivity and resistance to rust when sprayed with water in wet channels **(Liu et al. 2003)**. Five aluminium panels that come in size (122 cm width and 244 cm length) and thickness of 0.3 mm have been equipped.

Figure 2. Aluminum sheets with distribution of aspen pad.

The process of designing and cutting into 42 small sheets to be used in two-stage, and each stage had 21 sheets had dimensions (20 cm width and 80 cm length), as these sheets are installed in the first and second stages (21x21x80) cm drilled in acrylic by CNC, and silicone material was placed in the conduit to ensure that moist air did not transfer from the top of wet channel to dry channel as well as to prevent water leakage from the bottom into dry channel.

2.3 Measuring System

The Measuring Instruments have been connected to an Arduino mega 2560 microcontroller to display the results of water flow rate **(Yoeseph et al., 2022)**, water temperature **(Permana et al., 2021)**, relative humidity, and air temperature **(Mihai et al., 2016)** every

two minutes on an Excel sheet on the computer. The Measuring Instruments used are shown in **Table 1** as:

Table 1. Measuring Instruments.

Instruments	Type	Accuracy	Operation range
Temperature and humidity of air	DHT22	$<\pm 0.5$ °C $\pm 2\%$ RH	-40 to 80 °C 0-100% RH
Hot wire anemometer	YK-2005AH	$\pm 5\%$	0.2 to 20 m/s
Water flowmeter	YF-S201	$\pm 3\%$	0-30 lpm
Water temperature	DS18B20	± 0.5 °C	-55 to 125 °C

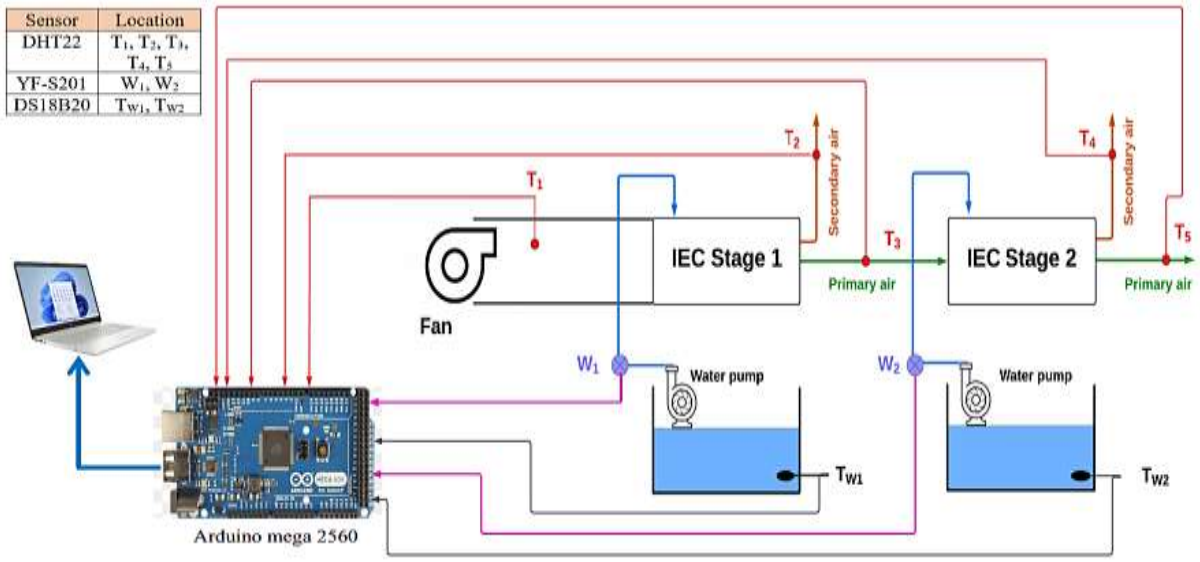

Figure 3. Schematic diagram of the measurement system

2.4 EXPERIMENTAL PROCEDURE

The blower (centrifugal type) is switched on to pump the hot outside air into the air duct, where the airflow into the duct is in the range of 150 CMH to 350 CMH, and in five steps, each step is 50 CMH more than the other. The blower is controlled by controlling the rotating speed of the motor through the voltage regulator connected to blower. Two water pumps are switched on to circulate water on the aspen pad. The water is sprayed through ten tubes distributed over ten wet channels through a large tube collecting and distributing water installed at the top of the duct. Each tube contains thirty nozzles to spray water on a cooling medium (aspen). A valve placed before the water flow sensor controls the amount of water. The amount of water pumped in each stage is (9, 16, and 20 lpm). To take a reading, start the water pump, set the amount of water flowing into the filling, and start with 9 lpm with this value of water fixed. The air quantity is set from 150 to 350 CMH at a rate of 50 CMH increment. After allowing 15 minutes for the system to stabilize, the results are taken for dry bulb temperature, relative humidity of outlet air from stage one, and air exit from stage two. This procedure is repeated with 16 lpm and 20 lpm water flow rate.

3. UNCERTAINTY ANALYSIS

The uncertainty of obtaining data collected during the experiment is determined by measurement accuracy and the kind of rig design **(Kline and McClintock, 1953)**. The most important influencing factors can be explained as follows:

1. Ambient air temperature and relative humidity
2. The type of sensor used and the location of its installation
3. The amount of water supplied and its temperature

To calculate the uncertainty in the obtained results **(Pantelic et al., 2018)** method is used in

$$\frac{j_G}{G} = \left[\left(\frac{\partial G}{\partial f_1}\frac{j_1}{G}\right)^2 + \left(\frac{\partial G}{\partial f_2}\frac{j_2}{G}\right)^2 + \left(\frac{\partial G}{\partial f_3}\frac{j_3}{G}\right)^2 + \cdots + \left(\frac{\partial G}{\partial f_n}\frac{j_n}{G}\right)^2\right]^{\frac{1}{2}} \quad (1)$$

The uncertainty of the independent parameters is given in **Table 2**.

Table 2. Uncertainty for all Independent Parameter.

Independent Parameter (f)	Uncertainty (j)	Independent Parameter (f)	Uncertainty (j)
Temperature (T)	$\pm$0.1 ℃	Air Velocity (v)	$\pm$0.001 m/s
Dry Channel Height (H)	$\pm$0.001 m	Relative Humidity (RH)	$\pm$2%
Dry Channel Width (W)	$\pm$0.0003 m	Water Flowrate (m)	$\pm$0.001 L/min

The cooling capacity equation presented in the performance can be written as:

$$Q_{cc} = \rho_{air}\, A\, v\, C_P\, \Delta T = N\, \rho_{air}\, H\, W\, v\, C_P\, \Delta T \quad (2)$$

where N is the number of primary air channels, and ΔT is the dry bulb temperature of inlet and outlet primary air. The experimental error in the cooling capacity calculation can be expressed in the following manner:

$$j_{Qcc} = \left[\left(\frac{\partial Q_{cc}}{\partial H}\, j_H\right)^2 + \left(\frac{\partial Q_{cc}}{\partial W}\, j_W\right)^2 + \left(\frac{\partial Q_{cc}}{\partial v}\, j_v\right)^2 + \left(\frac{\partial Q_{cc}}{\partial \Delta T}\, j_{\Delta T}\right)^2\right]^{\frac{1}{2}} \quad (3)$$

4. PARAMETRIC PERFORMANCE OF IEC

4.1 Wet Bulb Effectiveness

The ratio of the actual reduction in DBT of inlet air through the IEC system to the difference between DBT and WBT of ambient air is defined as wet-bulb effectiveness E. It is evaluated **(Wang et al., 2017; Putra et al., 2021)**:

$$E = \frac{T_{dry,a} - T_{dry,s}}{T_{dry,a} - T_{wet,a}} \quad (4)$$

4.2 Cooling Capacity

The cooling capacity (Q_{Se}) is calculated by recording the mass flow rate of air, the difference in dry-bulb temperature between inlet and outlet air, and air-specific heat **(Yousef et al., 2020; Kulkarni and Rajput, 2011)**.

$$Q_{Se} = \rho_{air} \forall \mathrm{C}_p \left(T_{dry,a} - T_{dry,s}\right) \quad (5)$$

4.3 Coefficient of Performance (*COP*)

The coefficient of performance of an air conditioning system is the ratio of cooling capacity (usable heating or cooling supplied) to the work required (*W)* **(Kabeel et al., 2017)**. Increased COPs imply lower operating costs **(Najam, 2017)**.

$$COP = \frac{Q_{se}}{W} \quad (6)$$

5. RESULTS AND DISCUSSION

This research aims to furnish a condensed overview and pragmatic discoveries, employing an aspen pad alongside an interposed aluminum sheet that demarcates the damp and arid passages. The outcomes will be exhibited encompassing the Dry Bulb Temperature (DBT) prevalent in both conduits, in conjunction with the relative humidity emanating from the moist channels, concerning a bifurcated configuration designated as the two-stage parallel flow cooler. Furthermore, an assessment will be conducted to gauge pertinent performance metrics, including cooling capacity, wet bulb effectiveness, Coefficient of Performance (COP), and water consumption. The parameters scrutinized in the present experimental inquiry are cataloged in **Table 3**.

Table 3. Range of investigated parameters.

Parameters	Range of Values
Inlet DBT of air (^{o}C)	43
Inlet WBT of air (^{o}C)	24.95
Air flow rate (CMH)	150-350
Water flow rate (lpm)	9, 16, 20
Inlet relative humidity (%)	23

Fig. 4 shows the change in the DBT value of secondary air passing through wet channels with its flow rate in both stages (first and second). The total air is divided into 60% for dry channels and 40% for wet channels, and this division is applied to both stages. It was found that reasonable cooling was added to the air due to the aspen cooling pad because the aspen pad creates large amounts of surface area that are exposed to air being drawn from the ambient by the fan. Hence, a large surface area allows for quick evaporation with higher conductivity of aluminum sheets. The DBT of aluminum sheet decreases; thus, the DBT of air passing in wet channels falls.

A reasonably decreased air DBT through an aspen pad is the direct evaporative cooling effect in wet channels. It is also noted that when the amount of water spilled is 0.9 lpm per wet channel and the airflow is low, the WBT and DBT of air are low and vice versa.

The inversion that occurs at 9 lpm is a result of an increase in the amount of air supplied to the wet channel (43 ^{o}C), as the hot air will evaporate water droplets scattered on the cooling pad faster in a manner that is not commensurate with the amount of water supplied to wet channel and thus leads to lack of water droplets scattered on the cooling pad leads to passage of hot air through it without being completely cooled, and therefore DBT of air supplied from wet channels rises. Also, when the water flow reaches 16 lpm or 20 lpm, it leads to a rise in the secondary air temperature as a result of the high relative humidity inside the wet channels, which leads to the saturation of dry air with moisture and its inability to evaporate large amounts of water droplets. Thus, the air temperature rises by a small percentage in wet channels.

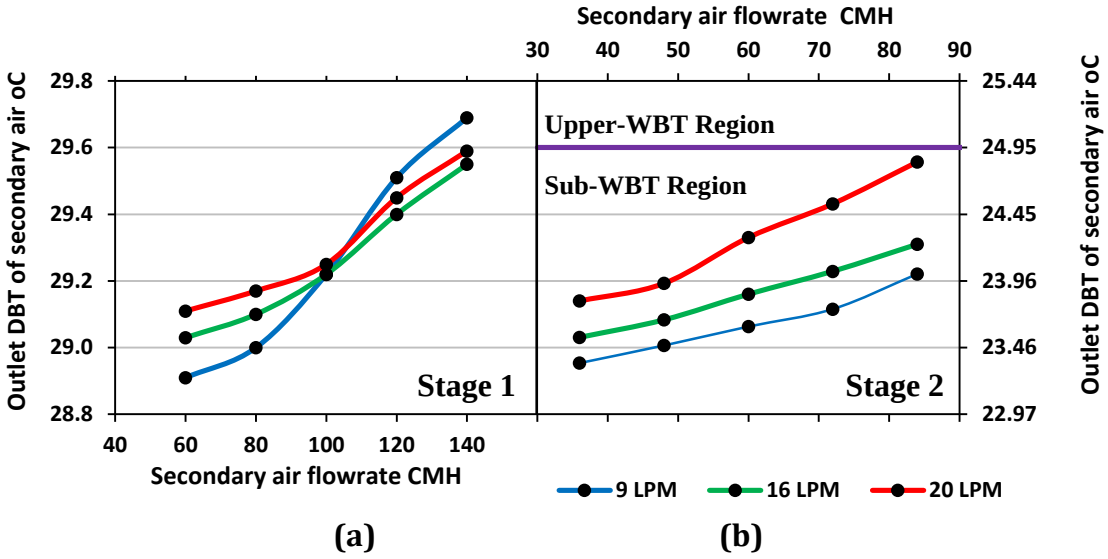

Figure 4. Variation of outlet DBT of secondary air with different air flow rates (a) Stage 1 and (b) Stage 2.

Fig. 5 indicates the DBT of primary air with the amount of airflow. It behaves like the secondary air, and the difference in DBT is very small due to the low air velocity supplied to both stages. **Fig. 6** presents a graphical representation of how the relative humidity exiting damp conduits fluctuates in response to alterations in the volume of secondary airflow and the dispensation of water via nozzles within these damp conduits. Elevated relative humidity levels are achieved by augmentation of air flux traversing the cooling pad within these moist conduits while maintaining a consistent water flow rate. This phenomenon can be elucidated through scientific reasoning. The reduction in relative humidity with increased air velocity during evaporative cooling can be attributed to "residence time." Residence time refers to the time air molecules spend in contact with the water surface in the evaporative cooling. When air moves at a higher velocity, it rapidly passes through the water source (such as a wet cooling pad or water spray).

This decreased contact time with the water surface means the air molecules have less time to interact and pick up moisture through evaporation. As a result, only a limited amount of water vapor is carried away by air, leading to lower humidity levels in the air stream. In other words, the air molecules are not given sufficient time to absorb the maximum possible moisture content from the water source due to their rapid movement. This phenomenon is especially pronounced when the airflow is high, as the air rushes past the water source quickly, not allowing enough time for significant evaporation. In contrast, when air moves more slowly, it spends more time in contact with the water source, allowing for greater evaporation and absorption of water vapor. This results in higher humidity levels in the air stream.

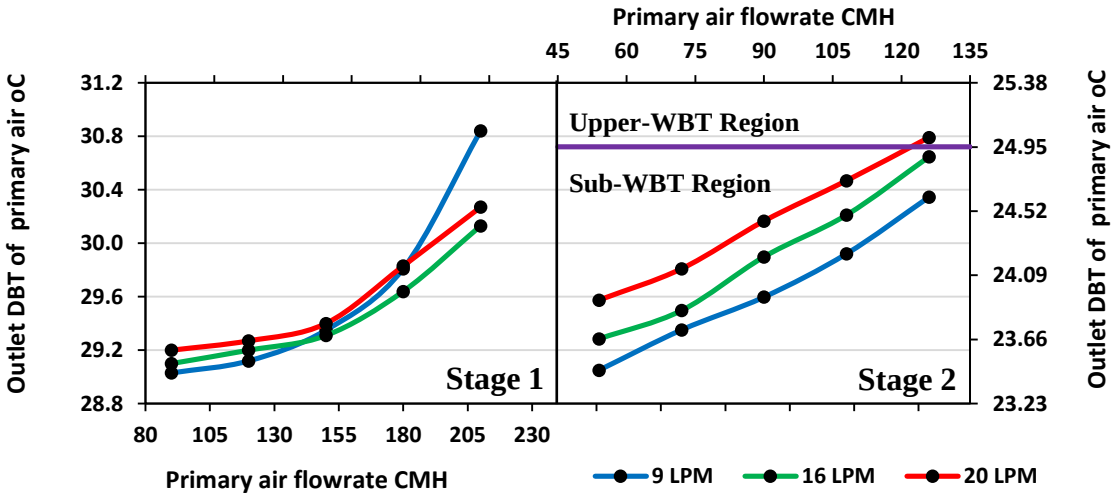

Figure 5. Variation of outlet DBT of primary air with different air flow rates.

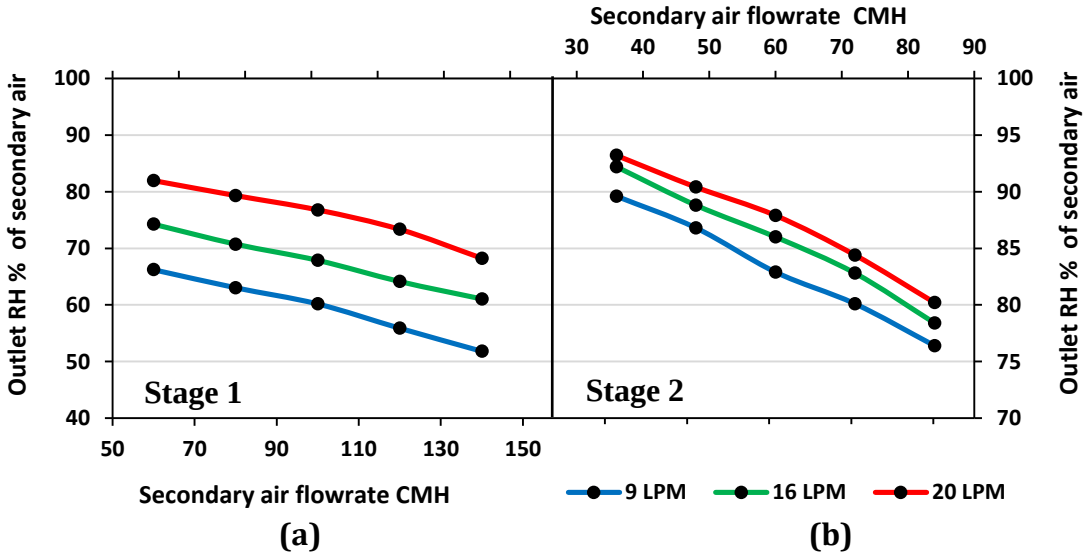

Figure 6. Variation of outlet relative humidity with secondary air flow rates (a) Stage 1 and (b) Stage 2.

Fig. 7 shows the water temperatures as the secondary air flow changes in wet channels. Whereas, in the case of a flow of 9 lpm, the water temperature decreases as a result of the direct evaporative cooling process, but an increase in the airflow to more than 100 CMH leads to a rise in water temperature due to the low amount of water supplied to wet channels. The water temperature is about two degrees lower than the secondary air temperature and does not reach the wet bulb temperature of the surrounding air.

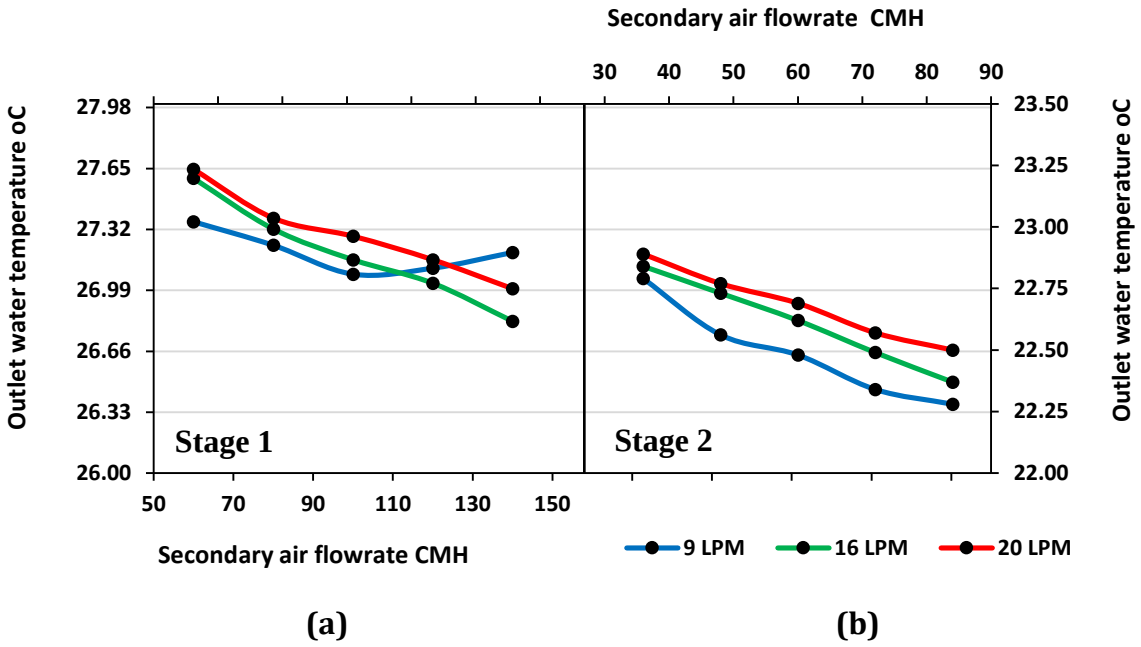

Figure 7. Variation of outlet water temperature with secondary air flow rates (a) Stage 1 and (b) Stage 2.

Fig. 8 Shows the total amount of energy consumed with the change in air and water flow. The energy consumption rate increases because the fan contains a special controller to determine airflow into the system. Increasing the water flow rate also leads to a rise in energy consumption rate, as the system's best performance was at a water flow of 9 lpm and an energy consumption rate not exceeding 100 W.

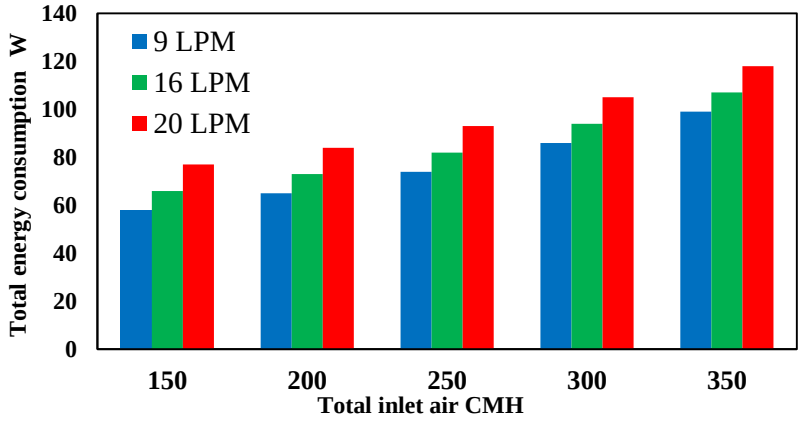

Figure 8. Variation of total energy consumption with total inlet air

.

Fig. 9 shows the relationship between the wet bulb effectiveness with water consumption and the primary air flow supplied from the cooler. At 9 lpm water flow rate, the water consumption ranges from 5 to 9 lpm at the best-wet bulb effectiveness. On the other hand, when the water supplied reaches 16 lpm leads to an increase in water consumption, but without an apparent effect on wet bulb effectiveness because the amount of water vapor in wet channels has increased.

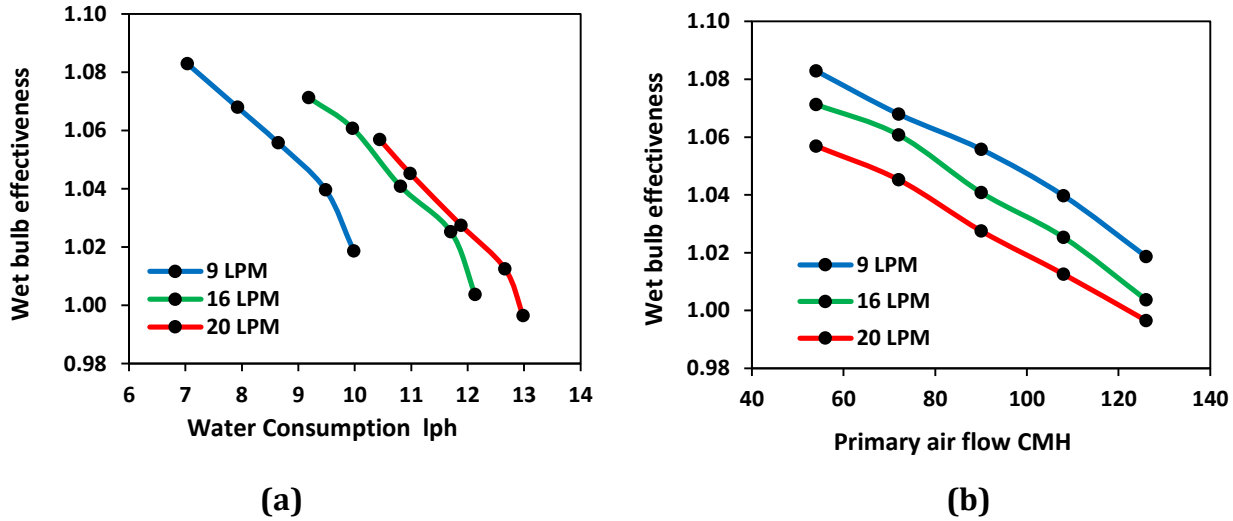

(a) **(b)**

Figure 9. Variation of wet bulb effectiveness with (a) water consumption and (b) primary air flow rates.

The evaporation and lowering of DBT of air in these channels will be limited. The wet bulb effectiveness calculated from Eq. (4) depends on the DBT of supplied primary air. The highest wet bulb effectiveness (1.083) was reported for 9 lpm of water flow at 54 CMH. The 20 lpm water flow rate lowers the wet bulb effectiveness value due to the high DBT of air supplied and low evaporative efficiency since the airflow to water sprayed ratio is small.

Fig. 10 illustrates the direct relationship between DBT and the flow rate of primary air with cooling capacity as obtained from Eq. (5). As the cooling capacity depends mainly on the amount of airflow more than it depends on the difference between ambient DBT and primary air supplied. The effect of the extraction ratio of 0.4 from total inlet air drawn into the wet channels is the most significant determinant of the cooling capacity values. The change in water flow rate from 9 to 20 lpm leads to a very slight change in air DBT, so the cooling capacity is almost equal in all air flows. **Fig. 11** depicts the alterations in the Coefficient of Performance (COP) contingent upon the Dry Bulb Temperature (DBT) of the air acquired from the dry channels. The COP is calculated using Eq. (6), leveraging the cooling capacity and the aggregate energy consumption. The highest COP value emerges under a water flow rate of 9 (lpm), ranging from 6.06 to 7.8. However, the escalation of water flow engenders a proportional augmentation in pump energy consumption. Consequently, the COP value experiences a reduction, noticeable within the context of both 16 and 20 lpm water flow rates. Furthermore, the influence of heightened primary airflow on the COP value is evident in **Fig. 11**.

This phenomenon is tied to the substantial influence of cooling capacity on the COP value. As the volume of air traversing the cooler augments, so does the cooling capacity, which, in turn, elevates the COP value. This correspondence between increased air volume and enhanced COP value underscores the pivotal role of cooling capacity as a determinant of COP performance.

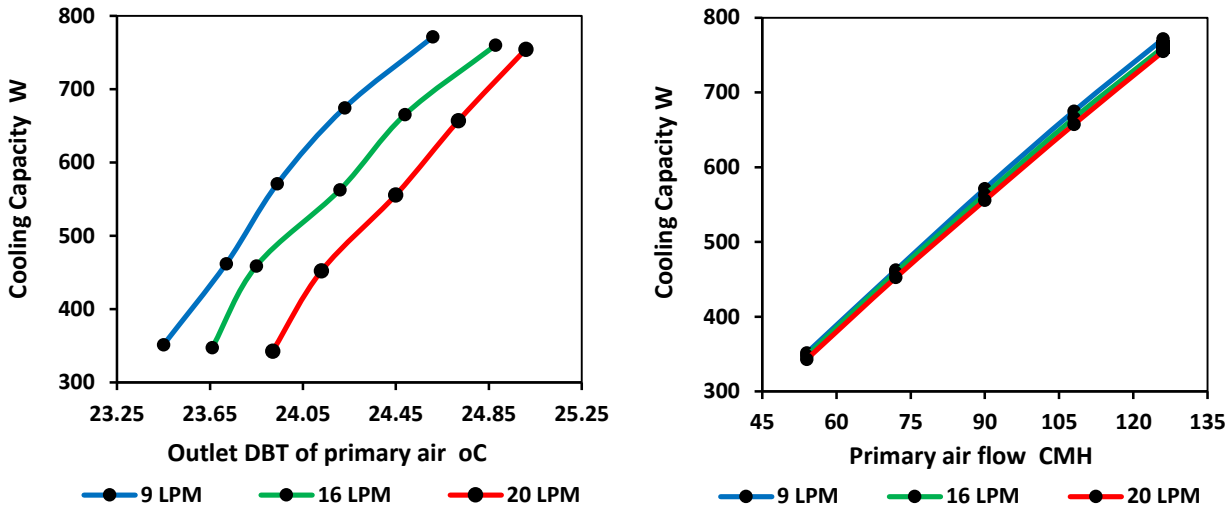

Figure 10. Variation of cooling capacity with (a) outlet DBT and (b) primary air flow in stage 2.

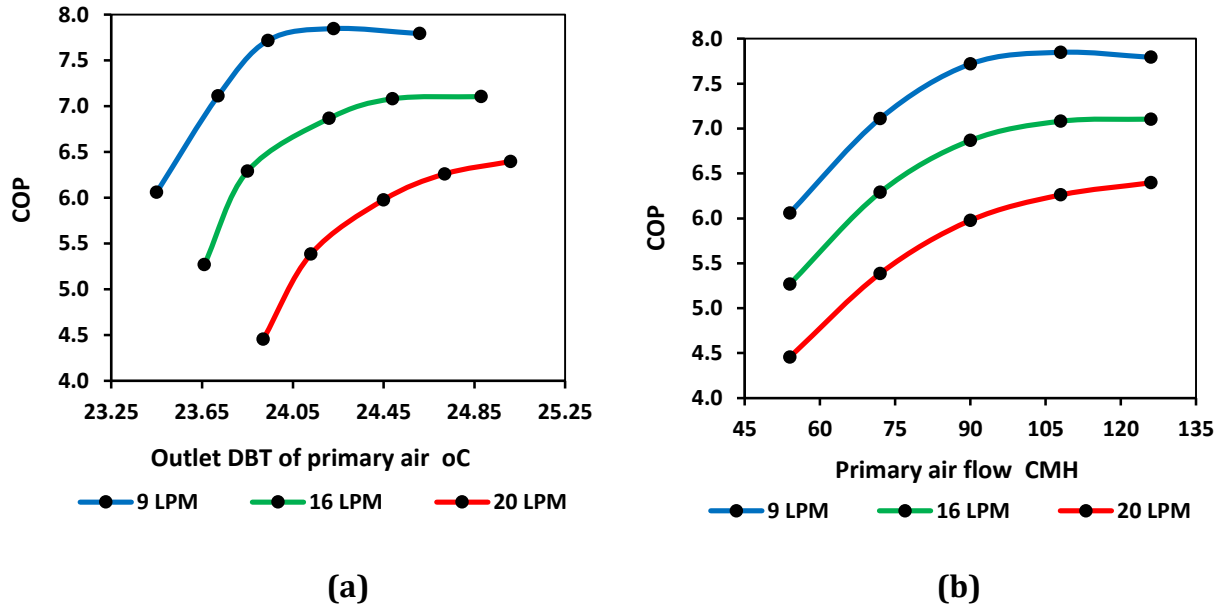

Figure 11. Variation of COP with (a) outlet DBT and (b) primary air flow in stage 2.

6. CONCLUSIONS

This study presents a significant advancement in the cooling technology field, particularly in Baghdad's demanding climate. The demonstrated capability of the two-stage parallel flow setup to achieve air dry bulb temperatures below the wet bulb temperature of the ambient air showcases its remarkable potential in overcoming conventional cooling limitations. However, it is crucial to highlight the sensitivity of the cooling system's performance to applying excess water onto the aspen pads within the wet channels. This finding underscores the importance of optimizing water usage for optimal cooler efficiency. This investigation has yielded notable outcomes, including the attainment of a minimum dry bulb temperature of 23.45°C for the primary air, the achievement of a remarkable coefficient of performance

(COP) of 7.8 for the two-stage parallel flow cooler, and the variability of wet bulb effectiveness values from 1.00 to 1.08. These findings were contingent upon the volume of air supplied into the system.

NOMENCLATURE

Symbol	Description	Symbol	Description
a	ambient	RH	Relative humidity
A	Area (m^2)	T	Temperature, °C
C_p	Specific heat capacity, kJ/kg. °C	s	supply air
CMH	Cubic meter per hour	se	sensible
COP	Coefficient of performance	v	Velocity of dry air, m/s
DBT	Dry bulb temperature	W	Total energy consumed, W
dry	dry temperature	WBT	Wet bulb temperature
E	Wet bulb effectiveness	wet	wet temperature
H	Dry channel height	W_{ch}	Dry channel width
lpm	Liter per minute	$\forall$	Volume rate of air, m^3/s
Q	Cooling capacity, W	ρ_{air}	Density of air, kg/m^3

REFERENCES

Alhosainy, A.H.M., and Aljubury, I.M.A., 2019. Two−stage evaporative cooling of residential building using geothermal energy. *Journal of Engineering,* 25(4), pp. 29–44. Doi:10.31026/j.eng.2019.04.03

Alklaibi, A.M., 2015. Experimental and theoretical investigation of internal two-stage evaporative cooler. *Energy Conversion and Management,* 95, pp. 140–148. Doi:10.1016/j.enconman.2015.02.035

Bai, Y., Yang, L., Zheng, S., and Huang, X., 2020. Discussion on the measures of achieving the sub-wet bulb temperature by evaporative cooling. *IOP Conference Series: Earth and Environmental Science,* 467(1), P. 012044. Doi:10.1088/1755-1315/467/1/012044

Boukhanouf, R., Alharbi, A., Ibrahim, H.G., Amer, O., and Worall, M., 2017. Computer modelling and experimental investigation of building integrated sub-wet bulb temperature evaporative cooling system. *Applied Thermal Engineering*, *115*, pp. 201-211. Doi:10.1016/j.applthermaleng.2016.12.119

Boukhanouf, R., Alharbi, A., Ibrahim, H.G., and Kanzari, M., 2013. Investigation of a sub-wet bulb temperature evaporative cooler for buildings. In *Sustainable Building Conference* (Vol. 13, No. 2013, pp. 70-79).

Duan, Z., Zhan, C., Zhang, X., Mustafa, M., Zhao, X., Alimohammadisagvand, B., and Hasan, A., 2012. Indirect evaporative cooling: Past, present and future potentials. *Renewable and sustainable energy reviews*, *16*(9), pp. 6823-6850. Doi:10.1016/j.rser.2012.07.007

El-Dessouky, H., Ettouney, H., and Al-Zeefari, A., 2004. Performance analysis of two-stage evaporative coolers. *Chemical Engineering Journal,* 102(3), pp. 255–266. Doi:10.1016/j.cej.2004.01.036

Hajidavalloo, E., 2007. Application of evaporative cooling on the condenser of window-air-conditioner. *Applied Thermal Engineering*, 27(11-12), pp. 1937-1943. Doi:10.1016/j.applthermaleng.2006.12.014

Hasan, A., 2010. Indirect evaporative cooling of air to a sub-wet bulb temperature. *Applied Thermal Engineering,* 30(16), pp. 2460–2468. Doi:10.1016/j.applthermaleng.2010.06.017

Hasan, A., 2012. Going below the wet-bulb temperature by indirect evaporative cooling: analysis using a modified ε-NTU method. *Applied Energy*, *89*(1), pp. 237-245. Doi:10.1016/j.apenergy.2011.07.005

Hashim, R.H., Hammdi, S.H., and Eidan, A., 2022. Evaporative cooling: a review of its types and modeling. *Basrah J Eng Sci*, *22*(1), pp. 36-47. Doi:10.33971/bjes.22.1.5

Heidarinejad, G., Bozorgmehr, M., Delfani, S., and Esmaeelian, J., 2009. Experimental investigation of two-stage indirect/direct evaporative cooling system in various climatic conditions. *Building and Environment*, 44(10), pp. 2073–2079. Doi:10.1016/j.buildenv.2009.02.017

Jassim, N.A., 2017. Performance enhancement of an air-cooled air conditioner with evaporative water mist pre-cooling. *Journal of Engineering*, *23*(1), pp. 48-62. Doi:10.31026/j.eng.2017.01.04

Jassim, N.A., and Haris, F.A.A., 2014. An investigation into thermal performance of mist water system and the related consumption energy. *Journal of Engineering*, *20*(9), pp. 108-119. Doi:10.31026/j.eng.2014.09.08

Kabeel, A.E., El-Samadony, Y.A.F., and Khiera, M.H., 2017. Performance evaluation of energy efficient evaporatively air-cooled chiller. *Applied Thermal Engineering*, *122*, pp. 204-213. Doi:10.1016/j.applthermaleng.2017.04.103

Kanzari, M., Boukhanouf, R., and Ibrahim, H.G., 2013. Mathematical modeling of a sub-wet bulb temperature evaporative cooling using porous ceramic materials. *International Journal of Industrial and Manufacturing Engineering*, 7(12), pp. 900–906. Doi:10.5281/zenodo.1089154

Kashyap, S., Sarkar, J., and Kumar, A., 2020. Comparative performance analysis of different novel regenerative evaporative cooling device topologies. *Applied Thermal Engineering*, 176, P. 115474. Doi:10.1016/j.applthermaleng.2020.115474

Kheirabadi, M., 2000. *Iranian cities: formation and development*. Syracuse University Press. Doi:10.35632/ajis.v17i3.2043

Kline, S.J., 1963. Describing uncertainties in single-sample experiments. *Mech. Eng.*, *75*, pp. 3-8.

Kulkarni, R.K., 2011. Theoretical performance analysis of indirect–direct evaporative cooler in hot and dry climates.

Lee, J., and Lee, D.Y., 2013. Experimental study of a counter flow regenerative evaporative cooler with finned channels. *International Journal of Heat and Mass Transfer*, 65, pp. 173–179. Doi:10.1016/j.ijheatmasstransfer.2013.05.069

Liu, H.J., Fujii, H., Maeda, M., and Nogi, K., 2003. Mechanical properties of friction stir welded joints of 1050–H24 aluminium alloy. *Science and technology of welding and joining*, *8*(6), pp. 450-454. Doi:10.1179/136217103225005598

Mahdi, A.H., and Aljubury, I.M.A., 2021. Experimental investigation of two-stage evaporative cooler powered by photovoltaic panels using underground water. *Journal of Building Engineering*, 44, P. 102679. Doi:10.1016/j.jobe.2021.102679

Mihai, B.O.G.D.A.N., 2016. How to use the DHT22 sensor for measuring temperature and humidity with the Arduino board. *Acta Uiversitatis Cibiniensis–Technical Series*, 68, pp. 22-25. Doi:10.1515/aucts-2016-0005

Nanyoo, 1987. Foshan Nanhai Nanyang Electrical Machinery and motor Co., Ltd. (www.ny-motor.com/en/)

Pantelic, J., Schiavon, S., Ning, B., Burdakis, E., Raftery, P., and Bauman, F., 2018. Full scale laboratory experiment on the cooling capacity of a radiant floor system. *Energy and Buildings*, 170, pp. 134-144. Doi:10.1016/j.enbuild.2018.03.002

Paul, S.D., Jain, S.K., Das Agrawal, G., and Misra, R., 2021. Performance Analysis of Two-Stage Evaporative Cooler: A Review. *Fluid Mechanics and Fluid Power: Proceedings of FMFP 2019*, pp.701-707. Doi:10.1007/978-981-16-0698-4_77

Permana, A.N., Wibawa, I.M.S., and Putra, I.K., 2021. DS18B20 sensor calibration compared with fluke hart scientific standard sensor. *International Journal of Physics and Mathematics*, *4*(1), pp. 1-7. Doi:10.31295/ijpm.v4n1.1225

Porumb, B., Ungureşan, P., Tutunaru, L.F., Şerban, A., and Bălan, M., 2016. A review of indirect evaporative cooling technology. *Energy procedia*, *85*, pp. 461-471. Doi:10.1016/j.egypro.2015.12.228

Putra, N., Sofia, E., and Gunawan, B.A., 2021. Evaluation of indirect evaporative cooling performance integrated with finned heat pipe and luffa cylindrical fiber as cooling/wet media. *Journal of Advanced Research in Experimental Fluid Mechanics and Heat Transfer*, *3*(1), pp.16-25. www.akademiabaru.com/submit/index.php/arefmht/article/view/3757

Riangvilaikul, B., and Kumar, S., 2010. Numerical study of a novel dew point evaporative cooling system. *Energy and Buildings*, 42(11), pp. 2241–2250. Doi:10.1016/j.enbuild.2010.07.020

Taleb, A.M., and Nima, M.A, 2021. Experimental investigation of thermal performance of aluminum foil coated with polyester in a direct evaporative cooling system. *Journal of Engineering,* 27(4), pp. 1–15. Doi:10.31026/j.eng.2021.04.01

Wang, F., Sun, T., Huang, X., Chen, Y., and Yang, H., 2017. Experimental research on a novel porous ceramic tube type indirect evaporative cooler. *Applied Thermal Engineering*, *125*, pp.1191-1199. Doi:10.1016/j.applthermaleng.2017.07.111

Xu, P., Ma, X., Zhao, X., and Fancey, K.S., 2016. Experimental investigation on performance of fabrics for indirect evaporative cooling applications. *Building and Environment*, *110*, pp. 104-114. Doi:10.1016/j.buildenv.2016.10.003

Yoeseph, N.M., Purnomo, F.A., and Hartono, R., 2022, February. Lora-based IOT sensor node for real-time flood early warning system. In *IOP Conference Series: Earth and Environmental Science* (Vol. 986, No. 1, P. 012060). IOP Publishing. Doi:10.1088/1755-1315/986/1/012060

Zhao, X., Liu, S., and Riffat, S.B., 2008. Comparative study of heat and mass exchanging materials for indirect evaporative cooling systems. *Building and Environment*, 43(11), pp. 1902–1911. Doi:10.1016/j.enbuild.2003.10.010

Zhou, Y., Yan, Z., Gao, M., Dai, Q., and Yu, Y., 2021. Numerical investigation of a novel plate-fin indirect evaporative cooling system considering condensation. *Processes*, *9*(2), P. 332. Doi:10.3390/pr9020332